Cement & Concrete Composites 34 (2012) 642–649

Contents lists available at SciVerse ScienceDirect

Cement & Concrete Composites

journal homepage: www.elsevier.com/locate/cemconcomp

Hydration and properties of nano-TiO_2 blended cement composites

Jun Chen [a,b], Shi-cong Kou [a], Chi-sun Poon [a,*]

[a] Department of Civil and Structural Engineering, The Hong Kong Polytechnic University, Hung Hom, Hong Kong
[b] Department of Building Innovation Technology, Shanghai Research Institute of Building Science, Shanghai, China

ARTICLE INFO

Article history:
Received 1 September 2010
Received in revised form 15 February 2012
Accepted 18 February 2012
Available online 24 February 2012

Keywords:
Cement
Nano-TiO_2
Hydration
Physical properties

ABSTRACT

Two types of nano-TiO_2 particles were blended into cement pastes and mortars. Their effects on the hydration and properties of the hydrated cement pastes were investigated. The addition of nano-TiO_2 powders significantly accelerated the hydration rate and promoted the hydration degree of the cementitious materials at early ages. It was demonstrated that TiO_2 was inert and stable during the cement hydration process. The total porosity of the cement pastes decreased and the pore size distribution were also altered. The acceleration of hydration rate and the change of microstructure also affected the physical and mechanical properties of the cement-based materials. The initial and final setting time was shortened and more water was required to maintain a standard consistence due to the addition of the nano-TiO_2. The compressive strength of the mortar was enhanced, practically at early ages. It is concluded that the nano-TiO_2 acted as a catalyst in the cement hydration reactions.

1. Introduction

The interest on combining the use of photocatalysts together with construction and building materials has been growing rapidly in last decade. Nano-sized titanium dioxide (TiO_2) is the most widely used photocatalyst in this field due to its strong photocatalytic activity. Traditionally, TiO_2 has been used as a white pigment in paints, cosmetics and foodstuff because it is cheap, safe and chemically stable [1]. The versatile functions of TiO_2 which can serve both as photocatalytic materials and coating materials significantly promote its application together with interior furnishing materials and exterior construction materials, such as glass, wallpaper, ceramic tiles, cement mortars and paving blocks [2–6].

The fundamental mechanisms of photocatalysis have been systematically reviewed [7,8]. The basic principle can be summarized as follows: when TiO_2 is exposed to UV irradiation, it can absorb photon energy equal to or larger than its band gap (3.2 eV, anatase), promoting electrons (e^-) to jump from the valence band to the conduction band. The activation of the electrons results in the generation of "holes" (h^+, electron vacancy) in the valence band. The electron–hole pairs may recombine in a short time to initiate redox reactions depending on ambient conditions. Several radicals, including $^{\cdot}OH$, $HO_2^{\cdot}$, O_2^{-} and $O^{\cdot}$, can be generated when water vapour and oxygen are present around the activated TiO_2. They can further react with substances adsorbed on the TiO_2 surface, resulting in the degradation of these substances.

The advance in photocatalytic materials research has established a solid foundation for its extended applications in the field of construction and building materials. There has been increasing interest in using cementitious materials as supporting media for the photocatalyst because of their strong binding property which can immobilize nano-TiO_2 powders within their matrices. TiO_2 powders can be conveniently mixed with cement based construction materials without additional treatments. The porous structure of the hardened cement pastes or mortars is also suitable for incorporating the TiO_2 particles and other photo-oxidation products. The major applications of the TiO_2 based photocatalytic cementitious materials include air pollution remediation, self-cleaning and self-disinfection [9–11]. These materials are preferred to be applied on external building surfaces and concrete pavements because the relatively flat configurations of these surfaces can facilitate the exposure of the photocatalysts to sun-light. It is expected that the photocatalytic cementitious material coated buildings can maintain their aesthetic appearance and reduce urban air pollution level at the same time.

However, as a new functional material, although the depollution and self-cleaning performance has been extensively discussed [12,13], little research has been conducted to examine the effects of nano-TiO_2 on the inherent properties of the hardened cement pastes. In addition, it is still controversial whether the added nano-TiO_2 particles have certain pozzolanic activity or they are only fine non-reactive fillers. Therefore, for potential large scale applications, the basic properties of the nano-TiO_2 modified cement pastes must be clearly identified.

Previously the authors have reported the influence of the microstructure of the hardened cement pastes on the photocatalytic

* Corresponding author. Tel.: +852 2766 6024; fax: +852 2334 6389.
E-mail address: cecspoon@polyu.edu.hk (C.-s. Poon).

0958-9465/$ - see front matter © 2012 Elsevier Ltd. All rights reserved.
doi:10.1016/j.cemconcomp.2012.02.009

pollution degradation reaction [14]. The aim of this paper is to present the results of our further study on the influence of nano-TiO_2 particleson the properties of the hardened cement pastes. Reference samples (pure cement) and cement/TiO_2 composite samples containing up to 10% TiO_2 (in addition) by the weight of cement were prepared. Hydration heat measurements, thermal gravimetric analyses (TGA), X-ray diffraction examinations (XRD) and mercury intrusion porosimetric measurements (MIP) were conducted. Additionally, the macro-properties, such as standard consistence, setting time and compressive strength of the cement pastes were also tested.

2. Experimental

2.1. Materials and sample preparation

Both the pastes and mortars were made in the laboratory for this study. Two kinds of TiO_2 with different crystal phase compositions, P25 (75% anatase and 25% rutile, Degussa, Germany) and Anatase (99% anatase, Sigma–Aldrich, USA), were added to an Ordinary Portland cement (OPC, ASTM type I) produced by Green Island Cement Limited of Hong Kong. The primary particle size of P25 and Anatase were 21 nm and 350 nm respectively, and their BET surface area were 58.8 $m^2 g^{-1}$ and 7.5 $m^2 g^{-1}$ respectively, measured using a Micrometritics ASAP2010 system. The chemical compositions and the Bogue composition of the cement are listed in Table 1. The specific surface area and the specific gravity of the cement were 3530 $cm^2 g^{-1}$ and 3160 kg m^{-3} respectively. Fine natural river sand (mainly quartz sand) sourced from the Pearl River was used in the mortar preparation. The saturated surface dry density of the sand was 2650 kg m^{-3}.

For the study of hydration products, cement paste samples were prepared by mixing cement, water with P25 and Anatase separately using a mechanical mixer. The water/cement ratio was kept at 0.35 and the amount of photocatalysts added was 5% and 10% of the total weight of cement. A smooth and well blended paste was produced and cast into steel moulds (dimensions $40 \times 40 \times 40$ mm). The moulds were vibrated by a vibrating table to ensure thorough compaction. After that, the paste samples were cured in an environmental chamber at 25 °C and 95% RH for 24 h. After one day, the hardened pastes were removed from their moulds and placed back into the same chamber at the same conditions until the time of testing. Reference samples without TiO_2 addition were also made for comparison. For the study of compressive strength, cement mortar (dimensions $50 \times 50 \times 50$ mm) were prepared in accordance with ASTM C109 [15] using a cement to sand ratio of 1:2.75 and a water to cement ratio of 0.485.

2.2. Testing

2.2.1. Determination of heat of hydration

The rates of heat evolution and the heat of hydration were measured using a JAF isothermal conduction calorimeter. The calorimeter had a heat sink maintained at constant temperature and the heat generated by the chemical reaction from the cement hydration flows through a known thermal path. There was an interface module which allowed the heat evolution to be recorded in the form of a calibration curve. The samples were prepared by mixing cement, TiO_2 and waste in polyethylene bags. The mix proportions for this study are given in Table 2. The measurement was conducted over a 72 h period.

2.2.2. Determination of non-evaporable water content

The non-evaporable water, defined as the mass loss due to decomposition between water boiling temperature and 900 °C, can be used as a relative measurement of the degree of hydration of the Portland cement [16,17]. The content of the chemically bound water in the hardened cement pastes was evaluated by TG analysis. The samples prepared for this study were obtained by crushing the hydrated cement pastes using a compression machine after 3, 7 and 28 days of curing. To stop hydration and prevent carbonation, the crushed pieces were soaked in acetone and stored for a minimum of 1 week. The crushed and grinded samples were heated at a rate of 10 °C min^{-1} up to 1000 °C under an Argon atmosphere using a TG/DSC analyzer (STA 449C Jupiter, NETZSCH, Germany). The content of non-evaporable water was calculated from the weight loss between 120 °C and 900 °C.

2.2.3. Semi-quantitative X-ray diffraction analysis

The hydration products of the nano-TiO_2 blended cement pastes and their relative quantities were determined by a semi-quantitative XRD measurement. Small pieces of crushed sample were ground into fine powder using a mechanical ballmill. 0.111 g of ZnO (AR grade) was added into 1.000 g weighted ground powder, and then the mixtures were allowed to passed through a 125 μm sieve three times to ensure the two materials were thoroughly mixed. The X-ray diffraction data was collected by an X-ray diffractometer (Bruker D8 Discover, Philips, The Netherlands) under ambient conditions. The samples were X-rayed from 5 to 65° (2θ) using monochromatic Cu K–α radiation, with a step size of 0.02°, and a count time of 2 s per step. The semi-quantitative X-ray diffraction analysis was conducted using the method proposed by Copeland and Bragg [18]. The ratio of the integrated intensities (I_0 and I_1) of the X-ray diffraction peaks of the two components in a mixture is proportional to the ratio of the weight fractions (w_0 and w_1) of those components.

$$\frac{I_1}{I_0} = k\frac{w_1}{w_0} \tag{1}$$

where k is a proportionality constant.

2.2.4. Determination of porosity and pore size distribution

MIP measurements were carried out to compare the porosity change of the hydrated cement pastes at the specified curing ages. The total porosity and the pore size distribution of the samples were analysed. The MIP measurements were carried out by using a mercury intrusion porosimeter (Poresizer9320, micromeritics, USA) with a maximum intrusion pressure of 210 MPa. A contact angle θ of 140° and a cylindrical pore geometry were assumed. The mercury intruded pore diameter d_p at an intrusion pressure of P_{In} was calculated by $d_p = -4\gamma\cos\theta/P_{In}$, where $\gamma = 0.483$ N m^{-1}, is the surface tension of mercury.

Table 1
Chemical composition of cement determined by X-ray fluorescence analysis and the Bogue composition.

Chemical composition											
Components	SiO_2	Al_2O_3	Fe_2O_3	CaO	MgO	K_2O	Na_2O	TiO_2	SO_3	P_2O_5	LOI
Mass%	21.62	5.15	3.50	66.06	2.16	0.48	0.24	0.37	2.54	0.10	0.64
Bogue composition											
Components	C_3S	C_2S	C_3A	C_4AF							
Mass%	57.7	18.5	7.7	10.7							

Table 2
Mix proportions for hydration heat experiment (P25 and Anatase were added separately).

Material	0% TiO_2	5% TiO_2	10% TiO_2
Cement (g)	30	30	30
Water (ml)	10.5	10.5	10.5
P25 (g)	N/A	1.5	3.0
Anatase (g)	N/A	1.5	3.0

2.2.5. Setting time and compressive strength test

The standard consistence and setting time of the cement pastes were determined using a Vicat apparatus according to the specification of BSEN 196–3 [19]. The compressive strength measurements of the cement mortars were conducted after 3, 7 and 28 days of curing in accordance with ASTM C109 [15].

3. Results and discussion

3.1. Heat of hydration of nano-TiO_2 blended cements

The heat evolution curves describing the rate of heat evolution for the cement/TiO_2 mixtures with 0%, 5% and 10% addition of nano-TiO_2 are presented in Fig. 1. Because the mixtures were prepared outside the calorimeter, the first heat evolution peak resulted from the fast hydration of tricalcium aluminate (C_3A) could not be recorded. As shown in the figures, the main peak occurred earlier for all the samples containing TiO_2 in comparison with the reference sample. The addition of the fine TiO_2 powders significantly increased the intensity of the heat peak and shortened its duration of occurrence. The increase of TiO_2 dosage from 5% to 10% enhanced these effects, but did not trigger a proportional increase of the heat release rate. Fig. 2 shows the curves of the total heat evolution during the first 72 h hydration. In correspondence with the trend of heat evolution rate, the incorporation of the nano-TiO_2 powders resulted in a greater cumulative heat release, particularly in the first 30 h. The acceleration of cement hydration reactions by inert or active ultra fine particles has been demonstrated by several studies [20–22]. It was proposed that those particles could act as potential heterogeneous nucleation sites for the hydration products and the grain boundary region was densely populated with nuclei and transformed completely early in the overall process of hydration [23–25]. In addition, the exothermic hydration process was accelerated more by P25 compared with Anatase, probably because the smaller particle size and larger surface area of P25 could provide more sites for the hydrates to deposit. This result indicates that the fineness and specific surface area of nano-mineral admixtures are key properties in determining the dissolution rate of cement compounds in the early stage of cement hydration.

3.2. Non-evaporable water content

Fig. 3 shows the TG curves of the pure cement sample and the 10% w/w P25 blended cement samples that had been hydrated for 3, 7 and 28 days. The content of the non-evaporable water bound in the cement pastes was determined as the weight loss between 120 °C and 900 °C on the TG curves. The non-evaporable water value for the samples incorporating 10% P25 was normalized with the mass fraction (0.909) of cement in the pastes, considering TiO_2 was a non-hydraulic additive. As shown in Fig. 4, the non-evaporable water content increased with hydration age. Dosing nano-TiO_2 powders into the cement pastes significantly enhanced the amount of chemically bound water, especially at the early curing ages, indicating that the hydration reactions were accelerated.

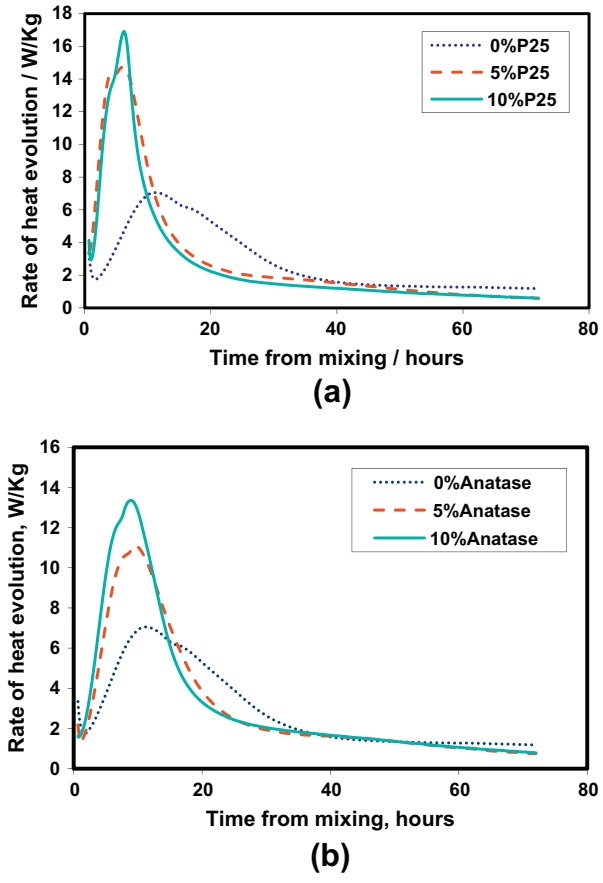

Fig. 1. Rate of heat evolution for different TiO_2 content: (a) P25, (b) anatase.

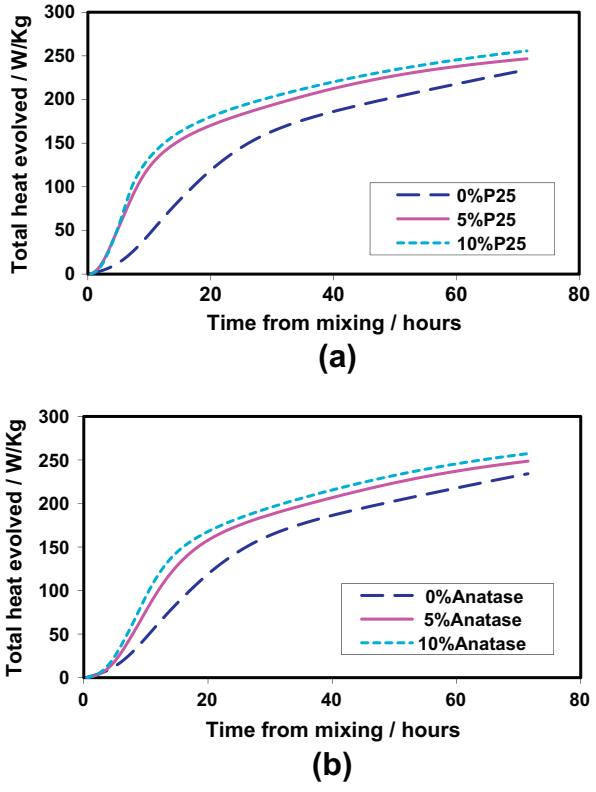

Fig. 2. Total heat of hydration for different TiO_2 content: (a) P25, (b) anatase.

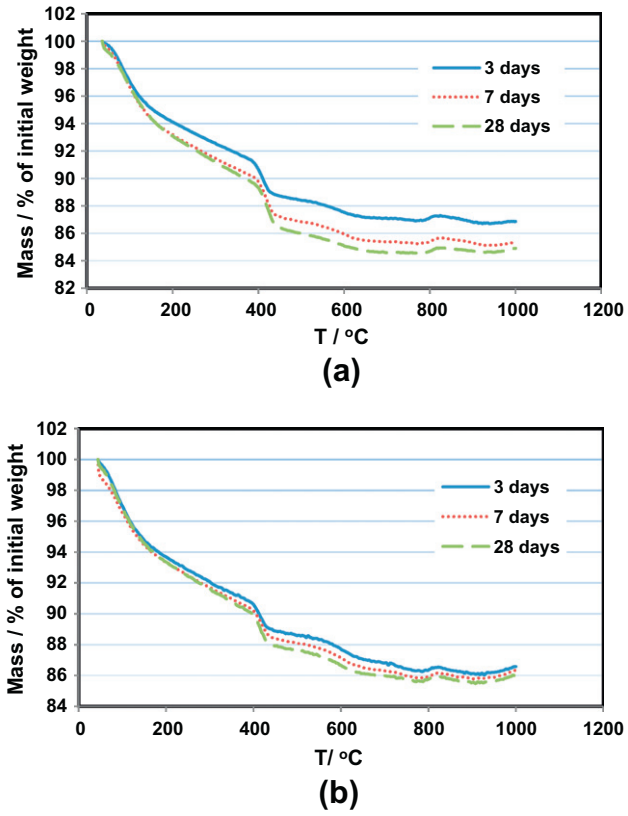

Fig. 3. TG diagrams: (a) pure cement sample hydrated at 3, 7 and 28 days, (b) sample containing additional 10% w/w P25 admixture hydrated at 3, 7 and 28 days.

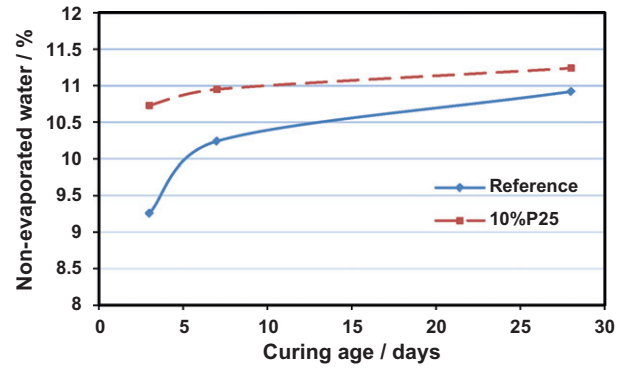

Fig. 4. Comparison of the content of non-evaporable water in pure cement paste and P25 blended cement paste at different curing age.

Based on this result together with the isothermal calorimetric measurements, it is suggested that nano-TiO_2 particles could accelerate the reaction rate during early hydration period and promote the formation and precipitation of hydration products.

3.3. Semi-quantitative XRD

To further investigate the effect of the nano-TiO_2 on the hydration of the cement pastes, chemical compositions and microstructure analysis were carried out. The XRD patterns of the 10% w/w P25 blended cement sample hydrated for 3, 7 and 28 days are shown in Fig. 5. MDI Jade 5.0 was used to identify the chemical compositions and to integrate the intensity of their corresponding peaks in the XRD pattern. Table 3 shows the calculation results of the relative mass ratios of TiO_2 at different curing ages. Except TiO_2 no other compounds containing elemental Ti can be identified. It seems that TiO_2 was inert and stable during the cement hydration process because and the variation of TiO_2 content was very small. This finding confirms that the nano-TiO_2 acted as a non-reactive filler, ruling out the speculation that TiO_2 may be of certain pozzolanic activity [26].

3.4. Porosity and pore size distribution

The results of porosity test for the pure cement sample, P25 and Anatase blended samples after different curing age are shown in Table 4. It is clear that dosing nano-TiO_2 into cement pastes decreased the porosity. As shown in Fig. 6, the pore size distribution and the total pore volume were also modified. The nano-particles seem to act as effective fillers of voids. With hydration continued, the conglomerations containing the nano-particles as nucleus expanded and filled up the pore space around them gradually. The presence of these "nuclei" significantly accelerated the hydration reaction rate. Therefore, the hydrates accumulated rapidly and grew outwards into the water filled voids, resulting in the decrease in porosity. Moreover, it should be noticed that the reduction of porosity mainly occurred within the capillary pore range. Capillary pores are considered remnants of the water-filled space between the hydrated cement grains [23].

Increasing the dosage of the nano-TiO_2 from 5% to 10% did not lead to significantly lower total pore volumes after 28 days curing (Fig. 6). It is possible that the production of hydrates was so greatly stimulated, even by a small quantity of inert nano-particles, as to most of the capillary pores were filled up and the growth was confined by limited space after 28 days hydration. It is also interesting to note that the porosity of the anatase blended cement pastes was lower than the P25 blended samples. This was probably because P25 powders with smaller particle size were easier to be self-aggregated and created undisrupted pockets within the paste matrix, leading to higher porosity than the anatase blended samples.

3.5. Setting time and compressive strength

Table 5 presents the summary of the water demand and the setting time for different samples. The "water demand" represents the amount of water required to prepare a cement paste with standard consistency, which is specified in BS EN 196–3 [19]. As expected, the water demand of the nano-TiO_2 blended samples was higher than the pure cement sample. Blending cement with a high specific surface material would increase the wettable surface area and the amount of water adsorbed. The higher the dosage of TiO_2, the more water was needed. The setting time was shorter for the samples with higher nano-TiO_2 contents. This is because rapid consumption of free water speeded up the bridging process of gaps, and as a result, the viscosity increased and solidification occurred earlier. In addition, the addition of P25 particles which had larger surface area resulted a higher water demand and shorter setting time, which was consistent with the results of the hydration heat measurements. The quick set potential which is directly linked to the type of nano-TiO_2 and the amount of dosage also confirms that the doped nuclei with larger specified surface area can provide more sites for hydration products to interact, influencing the physical performance of the pastes.

The results of compressive strength development in relation to nano-TiO_2 addition levels are shown in Fig. 7. The compressive strength of the mortars was significantly improved at all ages due to the addition of nano-TiO_2. Using nano-TiO_2 with smaller particle size and increasing their dosage further enhanced the strength. However, it was found that the amount of super plasticizer added must be adjusted with the increase in the amount of TiO_2 to maintain the workability. Fig. 8 presents the comparison

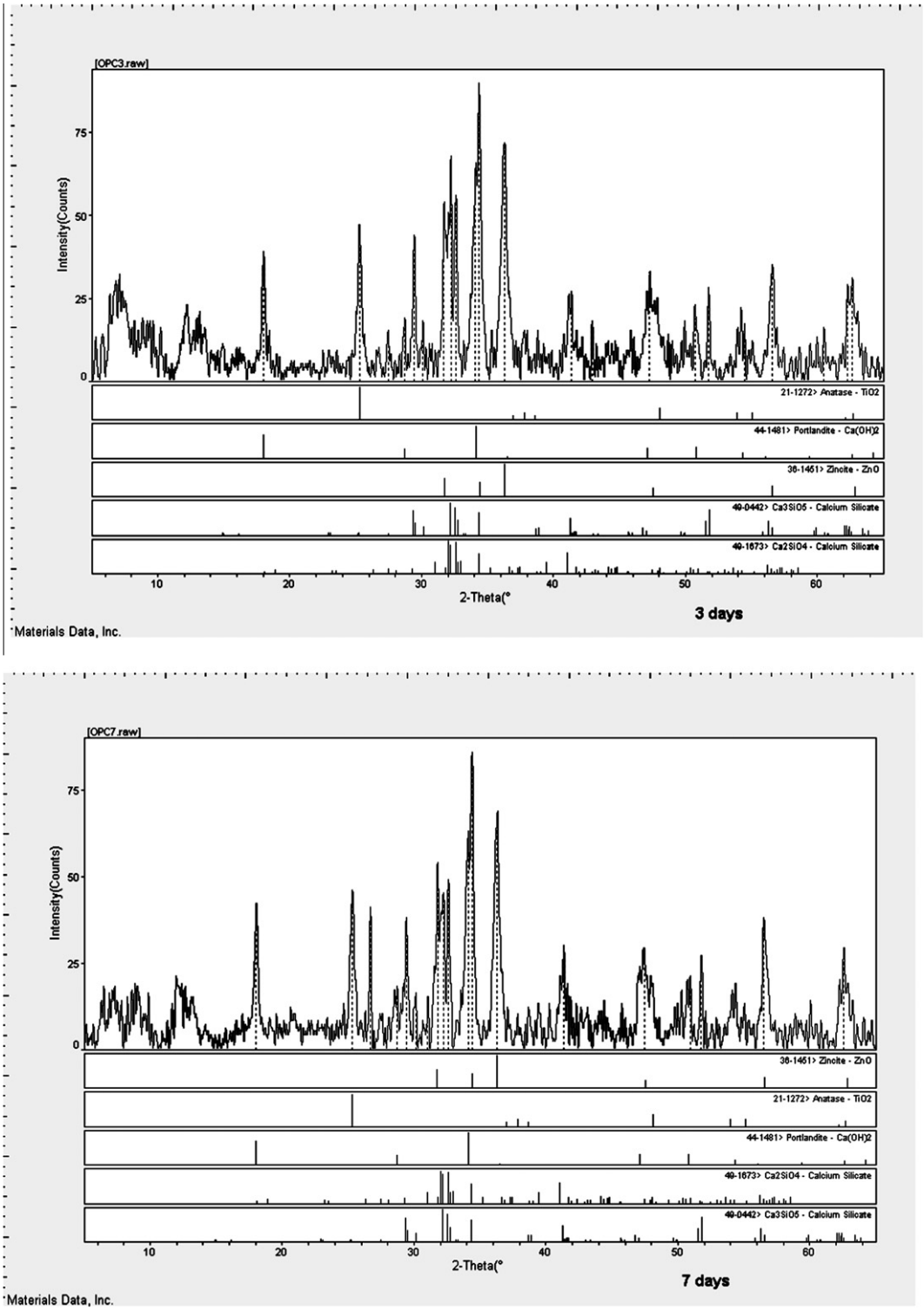

Fig. 5. XRD patterns of 10% w/w P25 blended pastes hydrated at 3, 7 and 28 days.

of the relative strength of the mortars. It can be seen that the ratios of all the samples decreased with increase in curing age. The rate of strength gain of the TiO_2 containing samples was higher at early ages than that at late ages. This was probably because the addition of nano-particles could only have an impact on the early hydration (C_3A and C_3S), and the much slower reaction of C_2S hydration which contributed to longer term properties of the hydrated cement pastes might be less affected.

3.6. Comparison between nano-TiO_2 and other nano-admixtures

Up till now, it is known that most of the work studying nano-particle admixtures in cement-based building materials has been focused on nano-silica that possesses certain pozzolanic activity [27]. Nano-silica has been shown to be able to accelerate the hydration reactions of C_3S and fly ash [28,29]; accelerate cement setting processes and decrease the setting time [30,31]; increase

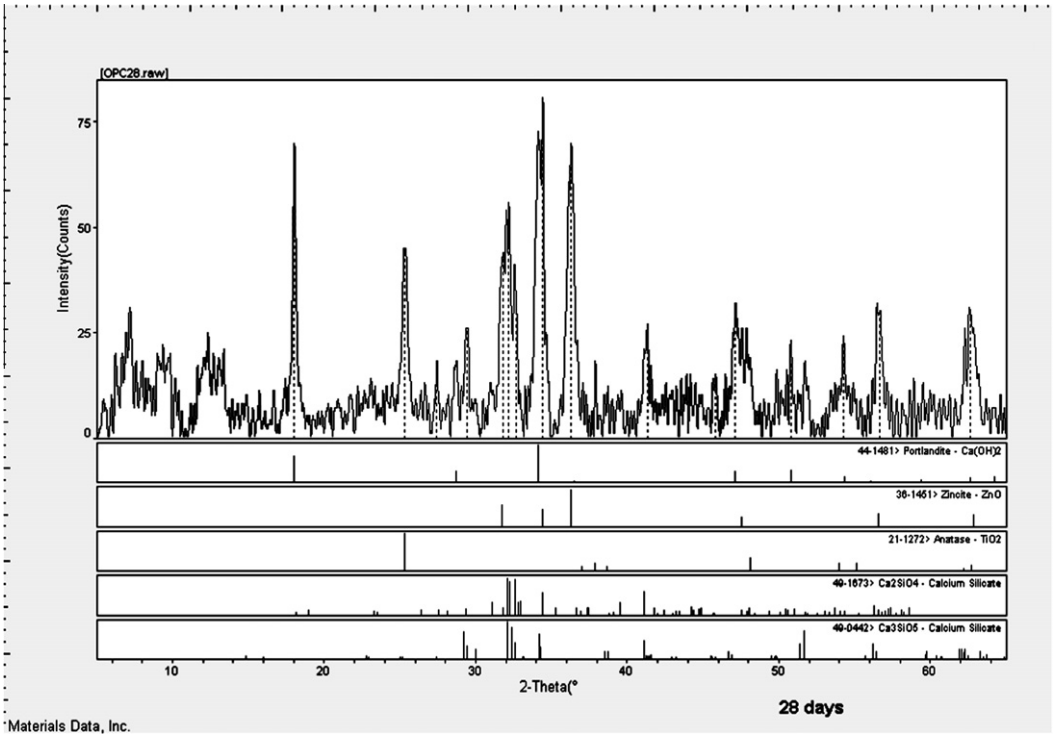

Fig. 5 (*continued*)

Table 3
Mass ratios of TiO_2 hydrated at 3, 7 and 28 days (with respect to the 3 days' data).

Substance	3 days	7 days	28 days
TiO_2	1	1.02	0.97

Table 4
Porosities of TiO_2 blended cement pastes after 3, 7 and 28 days curing.

Sample	Porosity (%, v/v)		
	3 days	7 days	28 days
Reference	22.92	22.31	20.55
5% P25	21.56	19.76	18.15
10% P25	20.56	19.31	17.54
5% Anatase	21.63	19.47	16.16
10% Anatase	20.83	17.19	16.10

the compressive strength of the cementitious system [29–32]. It has been demonstrated that the role of nano-SiO_2 is not only a pore filler to provide nucleation sites and modify the microstructure, but also an agent to promote pozzolanic reaction owing to its considerable surface activity [30,32,33]. In addition, there are also a few studies reporting the incorporation of nano-Fe_2O_3 and nano-Al_2O_3 could improve compressive and flexural strengths of concrete due to the compaction of interfacial transition zone [34,35].

Compared to nano-silica, nano-TiO_2 has similar effects on the cement hydration processes. However, as discussed before, TiO_2 is not a pozzolanic material. The results of this study showed that the change of pore structure and the improvement of compressive strength could only be attributed to the micro-filling effect of fine powders.

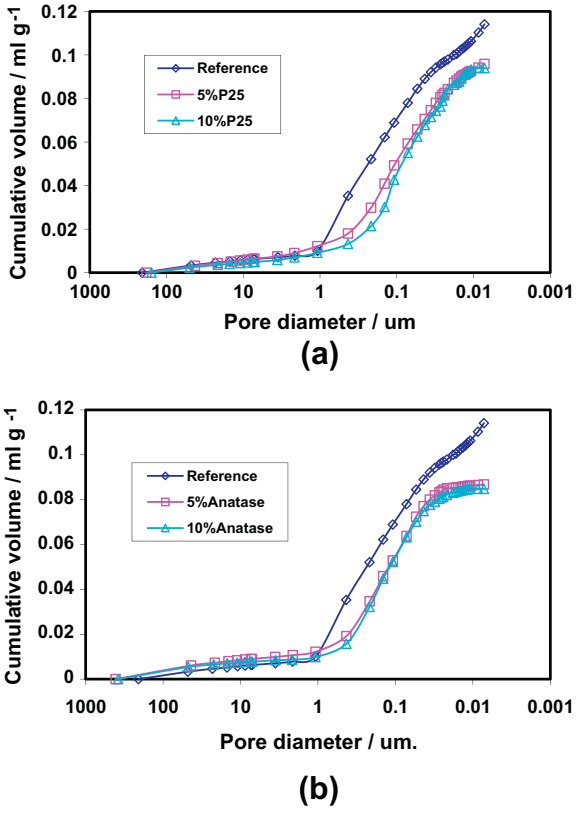

Fig. 6. Pore size distribution of TiO_2 blended cement paste hydrated at 28 days: (a) P25, (b) anatase.

Table 5
Physical properties of the nano-TiO_2 blended cement.

Sample	Water demand (%, w/w)	Setting time (min)	
		Initial	Final
Reference	26.0	160	240
5% P25	31.0	110	155
10% P25	36.0	100	145
5% Anatase	28.0	130	195
10% Anatase	30.0	125	185

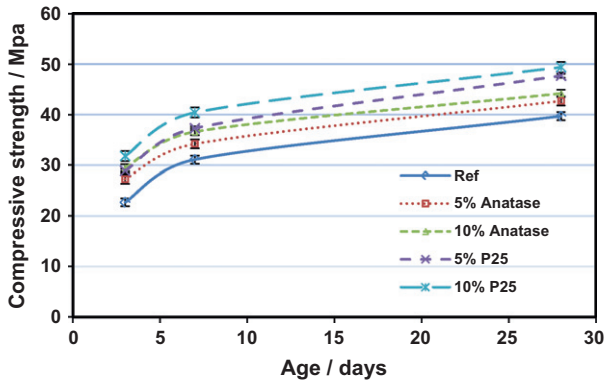

Fig. 7. Compressive strength development.

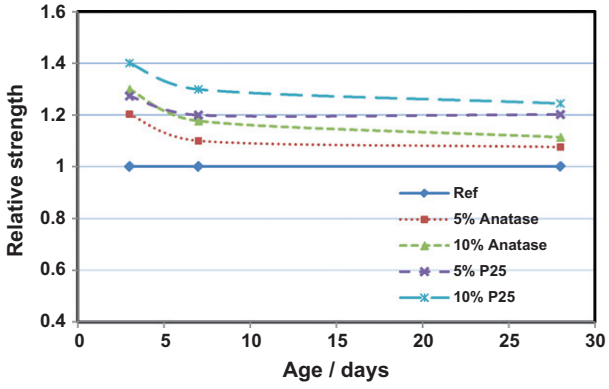

Fig. 8. Relative strength (with respect to the compressive strength of the reference sample at specified curing age).

4. Conclusions

The influence of adding nano-TiO_2 on cement-based materials was identified through experimental studies. The degree of hydration of at early hydration period was significantly enhanced by small dosages of nano-TiO_2 powder. TiO_2 was confirmed to be a non-reactive fine filler and had no pozzolanic activity. They acted as potential nucleation sites for the accumulation of hydration products. The total porosity of TiO_2 blended pastes was decreased and the reduction of pore volume mainly occurred mainly within the capillary pore range. The acceleration of hydration rate and the change in microstructure also affected the physical and mechanical properties of the cementitious materials. The smaller the nano-TiO_2 particles resulted in higher water demand and shorter setting time and the compressive strength of the mortars was significantly improved, practically at early ages. In conclusion, the nano-TiO_2 was not only a photocatalyst, it also had a catalytic effect in the cement hydration reaction when it was mixed into cement-based materials.

Acknowledgements

We gratefully acknowledge the financial support from The Hong Kong Polytechnic University. We also thank Miss Rebecca Smith for laboratory assistance.

References

[1] Fujishima A, Hashimoto K, Watanabe T. TiO_2 photocatalysis: fundamentals and applications. Japan: BKC Inc.; 1999.
[2] Paz Y, Luo Z, Rabenberg L, Heller A. Photo-oxidative self-cleaning transparent titanium dioxide films on glass. J Mater Res 1995;10:2842–8.
[3] Ichiura H, Kitaoka T, Tanaka H. Removal of indoor pollutants under UV irradiation by a composite TiO_2-zeolite sheet prepared using a papermaking technique. Chemosphere 2003;50(1):79–83.
[4] Wang R, Hashimoto K, Fujishima A, Chikuni M, Kojima E, Kitamura A, et al. Photogeneration of highly amphiphilic TiO_2 surfaces. Adv Mater 1998;10(2):135–8.
[5] Kawakami M, Furumura T, Tokushige H. NO_x removal effects and physical properties of cement mortar incorporating titanium dioxide powder. In: Baglioni P, Cassar L. editors. Proceedings RILEM symposium. France, RILEM Publications; 2007. p. 163–70.
[6] Chen J, Poon CS. Photocatalytic activity of titanium dioxide modified concrete materials – Influence of utilizing recycled glass cullets as aggregates. J Environ Manage 2009;90(11):3436–42.
[7] Agrios AG, Pichat P. State of the art and perspectives on materials and applications of photocatalysis over TiO_2. Appl Electrochem 2005;35(7):655–63.
[8] Fujishima A, Zhang X, Tryk DA. TiO_2 photocatalysis and related surface phenomena. Surf Sci Rep 2008;63(12):515–82.
[9] Maggos T, Plassais A, Bartzis JG, Vasilakos C, Moussiopoulos N, Bonafous L. Photocatalytic degradation of NO_x in a pilot street canyon configuration using TiO_2 – mortar panels. Environ Monit Assess 2008;136(1-3):35–44.
[10] Yuranova T, Sarria V, Jardim W, Rengifo J, Pulgarin C, Trabesinger G, et al. Photocatalytic discoloration of organic compounds on outdoor building cement panels modified by photoactive coatings. J Photochem Photobiol Chem 2007;188(2-3):334–41.
[11] Linkous CA, Carter GJ, Locuson DB, Ouellette AJ, Slattery DK, Smitha LA. Photocatalytic inhibition of algae growth using TiO_2, WO_3, and cocatalyst modifications. Environ Sci Technol 2000;34(22):4754–8.
[12] Strini A, Cassese S, Schiavi L. Measurement of benzene, toluene, ethylbenzene and o-xylene gas phase photodegradation by titanium dioxide dispersed in cementitious materials using a mixed flow reactor. Appl Catal B Environ 2005;61(1-2):90–7.
[13] Demeestere K, Dewulf J, DeWitte B, Beeldens A, Van Langenhove H. Heterogeneous photocatalytic removal of toluene from air on building materials enriched with TiO_2. Build Environ 2008;43(4):406–14.
[14] Chen J, Poon CS. Photocatalytic cementitious materials: influence of the microstructure of cement paste on photocatalytic pollution degradation. Environ Sci Technol 2009;43(23):8948–52.
[15] ASTM C109/109M-08. Standard test method for compressive strength of hydraulic cement mortars (using2-in. or [50-mm] cube specimens). Philadelphia: American Society for Testing and Materials; 2008.
[16] Escalante-Garcia JI. Nonevaporable water from neat OPC and replacement materials in composite cements hydrated at different temperatures. Cem Concr Res 2003;33(11):1883–8.
[17] Alarcon-Ruiz L, Platret G, Massieu E, Ehrlacher A. The use of thermal analysis in assessing the effect of temperature on a cement paste. Cem Concr Res 2005;35(3):609–13.
[18] Copeland LE, Bragg RH. Quantitative X-ray diffraction analysis. Anal Chem 1958;30:196–201.
[19] BSEN196-3. Methods of testing cements — Part 3: Determination of setting times and soundness. London: BSI Publications; 2005.
[20] Gutteridge WA, Dalziel JA. Filler cement the effect of the secondary component on the hydration of Portland cement. Cem Concr Res 1990;20:778–82.
[21] Poppe AM, Schutter GD. Cement hydration in the presence of high filler contents. Cem Concr Res 2005;35(12):2290–9.
[22] Kadri EH, Duval R. Hydration heat kinetics of concrete with silica fume. Construct Build Mater 2009;23(11):3388–92.
[23] Gartner EM, Young JF, Damidot DA, Jawed I. Hydration of Portland cement. In: Bensted J, Barnes P, editors. Structure and Performance of Cements. London: Spon Press, 2002.
[24] Lee BY, Thomas JJ, Treager M, Kurtis KE. Influence of TiO_2 nanoparticles on early C3S hydration. ACI Special, Publication 2009;267:35–44.
[25] Thomas JJ. A new approach to modeling the nucleation and growth kinetics of tricalcium silicate hydration. J Am Ceram Soc 2007;90(10):3282–8.
[26] Lackhoff M, Prieto X, Nestle FD, Niessner R. Photocatalytic activity of semiconductor-modified cement—influence of semiconductor type and cement ageing. Appl Catal B Environ 2003;43(3):205–16.
[27] Tao J. Preliminary study on the water permeability and microstructure of concrete incorporating nano-SiO_2. Cem Concr Res 2005;35(10):1943–7.
[28] Bjornstrom J, Martinelli A, Matic A, Borjesson L, Panas I. Accelerating effects of colloidal nano-silica for beneficial calcium–silicate–hydrate formation in cement. Chem Phys Lett 2004;392(1-3):242–8.

[29] Lin DF, Lin KL, Chang WC, Luo HL, Cai MQ. Improvements of nano-SiO_2 on sludge/fly ash mortar. Waste Manage 2008;28(6):1081–7.
[30] Ye Q, Zhang Z, Kong D, Chen R. Influence of nano-SiO_2 addition on properties of hardened cement paste as compared with silica fume. Construct Build Mater 2007;21(3):539–45.
[31] Senff L, Labrincha JA, Ferreira VM, Hotza D, Repette WL. Effect of nano-silica on rheology and fresh properties of cementpastes and mortars. Construct Build Mater 2009;23(7):2487–91.
[32] Li G. Properties of high-volume fly ash concrete incorporating nano-SiO_2. Cem Concr Res 2004;34(6):1043–9.
[33] Jo BW, Kim CH, Tae GH, Park JB. Characteristics of cement mortar with nano-SiO_2 particles. Construct Build Mater 2007;21(6):1351–5.
[34] Li H, Xiao HG, Ou JP. A study on mechanical and pressure-sensitive properties of cement mortar with nanophase materials. Cem Concr Res 2004;34(3):435–8.
[35] Li Z, Wang H, He S, Lu Y, Wang M. Investigations on the preparation and mechanical properties of the nano-alumina reinforced cement composite. Mater Lett 2006;60(3):356–9.